

# Modelling a Dune Field

A. R. Lima<sup>1</sup>, G. Sauermann<sup>1,2</sup>, H. J. Herrmann<sup>1,2</sup> and K. Kroy<sup>1</sup>

1) PMMH, Ecole Supérieure de Physique et Chimie Industrielles (ESPCI), 10, rue Vauquelin, 75231 Paris, Cedex 05, France

2) ICA-1, University of Stuttgart, Pfaffenwaldring 27, 70569 Stuttgart, Germany

---

## Abstract

We present a model to describe the collective motion of barchan dunes in a field. Our model is able to reproduce the observation that a typical dune stays confined within a stripe. We also obtain some of the pattern structures which resemble those observed from aerial photos which we do analyse and compare with the specific field of Laâyoune.

---

## 1 Introduction

A wide variety of dune shapes can be found in deserts, in coastal areas, on the sea-bottom [1], and even on Mars [2] and over one hundred different types of dunes have been classified by geomorphologists and their ancient predecessors so that some of them bear old arabic names. The shapes depend mainly on the amount of available sand and on the change in the direction of the wind over the year. If the wind blows steadily from the same direction throughout the year and there is not enough sand to cover the entire area, dunes called *barchans* develop having the shape of a crescent. They typically appear in huge fields of several hundred kilometers length stretching along coastlines and driven by trade-winds. A picture from a section of such a field is shown in Fig. 1.

Measurements of the relationship between height, width and length have been performed for instance in Peru or Morocco [3–8] and led to a good understanding of the barchan shape. In particular we know that the barchans move without changing their shape with a velocity which is inversely proportional to their height. However, the dynamics of dunes in a dune field has not yet been studied very much. In particular, there seems to be a contradiction between the fact that the barchans are not all of equal height and the stability of the dune field since when the dunes have different velocities they will eventually

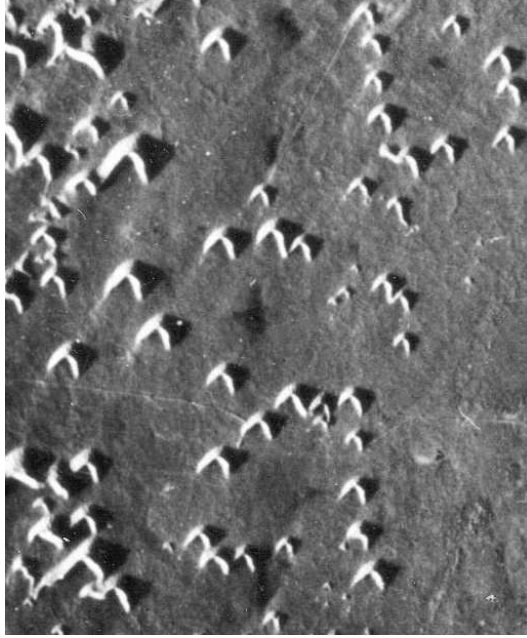


Fig. 1. Aerial photograph of a barchan dune field close to Laâyoune in Morocco. The photo clearly shows a correlation between the dunes in the lateral direction.

bump into one another. We do not yet understand the underlying stabilizing mechanism. Looking at the images in more detail also other questions arise. Are the relative positions of the dunes correlated? Do they form patterns? When dunes are getting closer they can interact through the non-local wind field or the sand flux between the dunes. In this work, we propose a simple model that defines the interaction between the dunes caused by the inter-dune sand flux. We neglect further effects of the wind field. The model predicts the time evolution of the entire field. It can reproduce the spatial correlations between the dunes that have been observed in the field, cf. Fig. 1. Furthermore, the model shows that the entire dune field does not broaden but stays focused. However, the stability of the dune field depends on the sand flux balance of a single dune, which is not well known so that we will have to make some simplifying assumptions.

## 2 Wind and sand flux

Sand is transported if the wind speed exceeds a certain threshold velocity. In equilibrium the amount of transported sand or the flux of sand  $q(u_*)$  can be expressed as a function of the shear velocity  $u_*$  [9]. The shear velocity  $u_*$  characterizes the turbulent boundary layer of the atmosphere and thus its well known logarithmic velocity profile  $v(z) = u_*/\kappa \ln z/z_0$ , where  $v(z)$  is the

wind speed at height  $z$  over the ground,  $\kappa \approx 0.4$  the universal von Kármán constant for turbulent flow, and  $z_0$  the roughness length of the surface. For shear velocities well above the threshold, e.g.  $u_* = 0.5 \text{ m s}^{-1}$ , the simplest sand flux relation, proposed by Bagnold [10], should give a reasonable prediction for the sand flux  $q$ ,

$$q = C_B \frac{\rho_a}{g} u_*^3, \quad (1)$$

where  $C_B \approx 2$  is a phenomenological constant [10–12],  $\rho_a = 1.225 \text{ kg m}^{-3}$  the density of air, and  $g = 9.81 \text{ m s}^{-2}$  the acceleration due to gravity. Using the bulk density  $\rho_s = 1650 \text{ kg m}^{-3}$  of a typical sand we can rewrite Eq. (1) into a relation for the volume flux  $\Phi$ ,

$$\Phi = \frac{q}{\rho_s} \quad (2)$$

For the discussion of the dune field dynamics we chose the shear velocity over the flat ground  $u_{*0} = 0.5 \text{ m s}^{-1}$  and obtain a volume sand flux  $\Phi_0$  of  $0.031 \text{ m}^2 \text{ s}^{-1}$ . Furthermore, we assume that the sand velocity  $v_s$  is proportional to the shear velocity  $u_*$  and choose a typical value of  $v_s = 5 \text{ m s}^{-1}$ .

### 3 Barchan dunes

A dune is characterized by a single scalar quantity, e.g. its width  $w$ , and its position  $(x, y)$  in the dune field. Further properties such as the height  $h$ ,

$$h = a w \quad (3)$$

or volume  $V$ ,

$$V = b w^3 \quad (4)$$

can be calculated using simple phenomenological formulas. Here, the parameters  $a = 0.09$  and  $b = 0.05$  have been obtained from field measurements [8].

The migration velocity  $v_d$  of a dune depends on its height  $h$  and the sand flux  $\Phi_b$  over the brink of the dune [10]. The latter can be calculated through Eq. (1) if the shear velocity at the brink is known. However, the dune itself disturbs the wind field such that it becomes stronger above the dune than over a flat ground. The ratio between the shear velocity over a flat ground  $u_{*0}$  and the shear velocity at the brink of the dune is called the “speed-up”  $n$ . This speed-up depends on the shape of the dune and mainly on the average

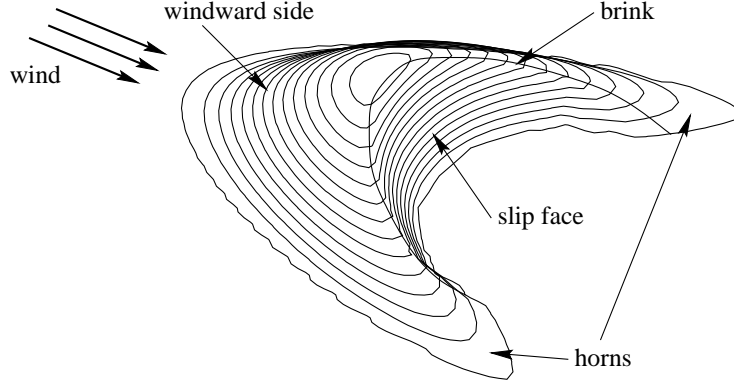


Fig. 2. Sketch of a barchan dune.

windward slope. A typical value for the speed-up over a sand dune is 1.4 [13,14]. Finally, we can write for the dune velocity  $v_d$ ,

$$v_d = \frac{\Phi_b}{h} = \frac{\Phi_0 n}{aw}. \quad (5)$$

We want to note that Eqs. (3) and (4) implicitly assume scale invariant dune shapes, which is an approximation that is only valid for large dunes, much larger than the minimal dune size [15,16].

The growth and shrinkage of a dune depends on the balance of in- and out-going sand fluxes. The sand flux that arrives from a upwind location, for instance a beach or other dunes, feeds the dune with new sand, whereas at the tip of the horns sand leaves the dune. The change of volume  $\dot{V}_i$  due to the in-flux  $\Phi(y)$  can be calculated by integrating over the dunes width,

$$\dot{V}_i = \int_0^w \Phi(y) dy. \quad (6)$$

The sand that leaves the dune at the horns gives rise to a loss of volume  $\dot{V}_o$  that is modeled by the following expression,

$$\dot{V}_o = w \Phi_0 (a_0 + a_1 w), \quad (7)$$

where  $a_0$  and  $a_1$  are parameters that depend on the complex processes occurring on the dune's surface and are not known a priori. Recent numerical calculations of the sand outflux from barchan dunes suggest that the outflux is nearly proportional to the dunes width and motivated the expression above [16].

For a stable dune, the gain and loss of volume must exactly compensate  $\dot{V}_i - \dot{V}_o = 0$ . The average inter-dune flux or influx  $\langle \Phi \rangle = f \Phi_0$  causes an average

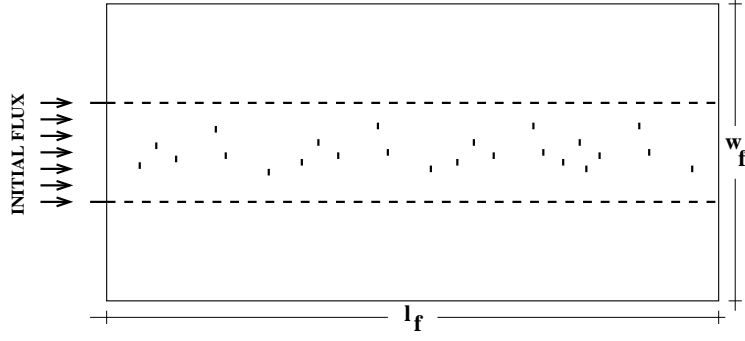


Fig. 3. Sketch of a dune field.

increase in volume,

$$\langle \dot{V}_i \rangle = w f \Phi_0, \quad (8)$$

where  $f$  defines the saturation of the inter-dune flux. Eqs. (7) and (8) define finally an average dune width  $\langle w \rangle$ ,

$$\langle w \rangle = \frac{f - a_0}{a_1}. \quad (9)$$

Using the average dune width  $\langle w \rangle$  and  $\gamma = a_1 \langle w \rangle / f$  as new parameters, instead of  $a_0$  and  $a_1$ , we can rewrite Eq. (7),

$$\dot{V}_o = w f \Phi_0 \left( 1 + \gamma \frac{w - \langle w \rangle}{\langle w \rangle} \right). \quad (10)$$

Finally, the change in volume  $\dot{V}$  of a dune can be obtained from Eqs. (6) and (10),

$$\dot{V} = \int_0^w \Phi(y) dy - w f \Phi_0 \left( 1 + \gamma \frac{w - \langle w \rangle}{\langle w \rangle} \right) \quad (11)$$

Typical values for  $f$  are of the order of 0.1, i.e. the inter-dune flux is far from being saturated.

#### 4 The barchan field

A barchan field of length  $l_f$  and width  $w_f$  as depicted in Figure 3 is composed of many dunes that migrate in the  $x$ -direction, the direction of the wind. The center of mass  $(x_i, y_i)$  of a dune is used to localize the dune  $i$  in the field. The dynamics of the dune field is described by the temporal change of the variables  $x_i$ ,  $y_i$ , and  $w_i$  which will be defined in the following.

From Eqs. (11) and (4) we obtain the change of the width of a dune, which depends on the inter-dune flux,

$$\dot{w}_i = b^{-1/3} \left[ \int_{y_i - w_i/2}^{y_i + w_i/2} \Phi(y) dy - w_i f \Phi_0 \left( 1 + \gamma \frac{w_i - \langle w \rangle}{\langle w \rangle} \right) \right]^{1/3} \quad (12)$$

The velocity of the dune in the wind direction is given in Eq. (5) and depends only on the width of the dune,

$$\dot{x}_i = v_d(w_i) = \frac{\Phi_0 n}{a w_i} \quad (13)$$

An inter-dune flux that is asymmetric in the lateral direction with respect to the center of mass  $y_i$  of the dune gives rise to a change in lateral position  $y_i$ ,

$$\dot{y}_i = \frac{V_i y_i + \int_{y_i - w_i/2}^{y_i + w_i/2} \tilde{y} \Phi(\tilde{y}) d\tilde{y}}{V_i + \int_{y_i - w_i/2}^{y_i + w_i/2} \Phi(\tilde{y}) d\tilde{y}} - y_i, \quad (14)$$

where  $V_i$  is the volume of the dune  $i$ .

Dunes can interact either due to the inter-dune flux or due to coalescence. The first case is defined by the equations above and the inter-dune sand flux  $\Phi(x, y)$  defined in the next section. For the latter case we define a characteristic distance of coalescence  $d_{\text{col}}$ . If two dunes become closer than this distance they are merged to a single dune. The mass is conserved by this process and the new position is calculated according to their centers of mass and relative volumes.

#### 4.1 The inter-dune sand flux in the field

The flux of sand in the field, i.e. between the dunes, is a complex problem and causes an interaction between the dunes. Dunes can act here as sources and sinks for the sand at the windward foot and at the horns, respectively. Furthermore, the position and width of the dunes changes in time and thus their influence on the inter-dune sand flux. We propose the following model for the inter-dune flux: First, the sand is convected with the constant velocity  $v_s$  in the wind direction. Secondly, a lateral movement is caused by diffusion and obeys a diffusion equation,

$$\frac{\partial \Phi}{\partial t} - D \frac{\partial^2 \Phi}{\partial y^2} = 0, \quad (15)$$

where the time scale of the diffusion process is connected to the transport in wind direction by the sand velocity  $v_s$ . Hence, we start solving the diffusion

equation at the influx-border  $x = 0$  of the field, where the sand flux is spatially constant. When integrating the solution forward in time by displacing its  $x$ -position we obtain the stationary solution of the two-dimensional inter-dune flux field  $\Phi(x, y)$ ,

$$v_s \frac{\partial \Phi}{\partial x} - D \frac{\partial^2 \Phi}{\partial y^2} = 0. \quad (16)$$

For each dune in the field, the flux  $\Phi_i$  is set to zero along the entire width of the dune (from  $y_i - w_i/2$  to  $y_i + w_i/2$ ). Then, at the horns (i.w. the positions  $y_i - w_i/2$  and  $y_i + w_i/2$ ) the outflux is imposed as two  $\delta$ -functions. Finally, the new dune mass is calculated by the in- and out-flux balance, Eq. (12).

#### 4.2 Initial configuration and Boundary conditions

The field is initialized with dunes at random positions until a certain density  $\rho_d$  is reached, which is a parameter of the model. The dune width is chosen between a minimum and a maximum width,  $w_{min} \leq w \leq w_{max}$ , having an average width  $\langle w \rangle = (w_{min} + w_{max})/2$ . From the initial density  $\rho_d$  we can define the rate  $r$  with which new dunes enter the field at the in-flux boundary,

$$r = W \rho_d v(\langle w \rangle), \quad (17)$$

where  $v(\langle w \rangle)$  is the dune velocity according to Eq. (5) and  $W$  is the width of the dune field, which is chosen to be only one third of the total simulation area, cf. Fig 3 where  $w_f = 3W$ . The width of the dunes that enter with the rate  $r$  at the influx boundary is chosen randomly as in the initial configuration. If a dune crosses the outflow boundary (at the right side of the field) it is removed from the simulation.

The inter-dune flux of sand  $\Phi$  is chosen to be constant between  $w_f/3 < y < 2w_f/3$  and zero outside. The constant influx is chosen to be  $\Phi = f\Phi_0$  and thus corresponds to an inter-dune flux of a dune field with average dune width  $\langle w \rangle$ , cf. Eq. (8). In the direction perpendicular to the wind ( $y$ -direction) periodic boundary conditions are used.

## 5 Numerical Scheme

The numerical scheme can be divided into several steps. First, the dune field is randomly initialized with dunes as discussed above. Then, an iterative calculation, forward in time, of the following steps is performed:

- New dunes are created with rate  $r$  at the left boundary, in the region  $w_f/3 < y < 2w_f/3$ .
- The new  $x$ -position of the dunes is calculated according to Eq. (13).
- If two dunes are closer than the coalescence distance  $d_{\text{col}} = 50$  m they are merged.
- The inter-dune sand flux is calculated from left to right on a discrete one dimensional grid in  $y$ -direction according to Eq. (16). The iteration is started at  $x = 0$  with a constant value of  $\Phi(y) = f\Phi_0$  for  $w_f/3 < y < 2w_f/3$  and zero outside. When the calculation forward in the wind direction reaches a dune, the flux is set to zero along the dune width and two discrete  $\delta$ -peaks are set at the horns of the dune as described above. Furthermore, the change in volume of the dune and its lateral movement according to Eqs. (12) and (14) are calculated.

The time step between the iteration cycles above has been chosen to be  $\Delta T = 1/12$  year.

## 6 Results

We are mainly interested in measuring how the dunes are distributed in the field, possible correlation between the positions of the dunes and understanding the confinement of the field on a stripe. We did simulations of our model for a field having a length of 50 km and a width of 12 km. The dunes enter the field only in the region between km 4 and km 8. The initial density of dunes in the field was chosen to be  $\rho_f = 10$  dunes/km<sup>2</sup>. We set the saturation of the flux to be  $f = 0.15$  which corresponds to a flux of  $\phi = 0.0046$  m<sup>2</sup>/sec.

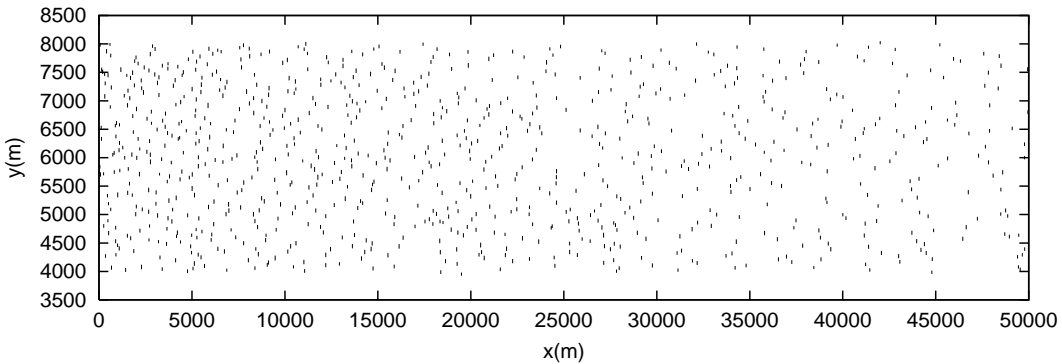


Fig. 4. Snapshot of the simulation of the field.

In fig. 4 we see a typical simulation of the dune field. It stays confined inside a stripe. The dune density slowly decreases in direction of the wind. This can be seen quantitatively in Fig.5 where the density averaged over the  $y$  direction is plotted over the  $x$ -axis ( $x$  and  $y$  directions are defined in fig. 4)



in a semilogarithmic plot. We recognize for large  $x$  a logarithmic decay of the form  $\rho \propto \ln x$ .

The situation seen in fig. 4 is a stationary state. As seen in fig. 6 the average size of the dunes fluctuates around a value that is constant in time and except for a short transient at early times also the number of dunes is essentially constant in time.

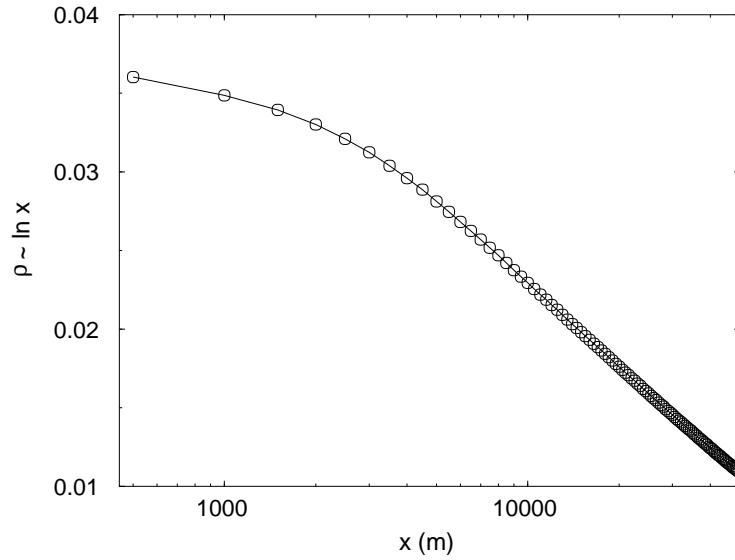


Fig. 5. Time averaged density of the dunes along the field.

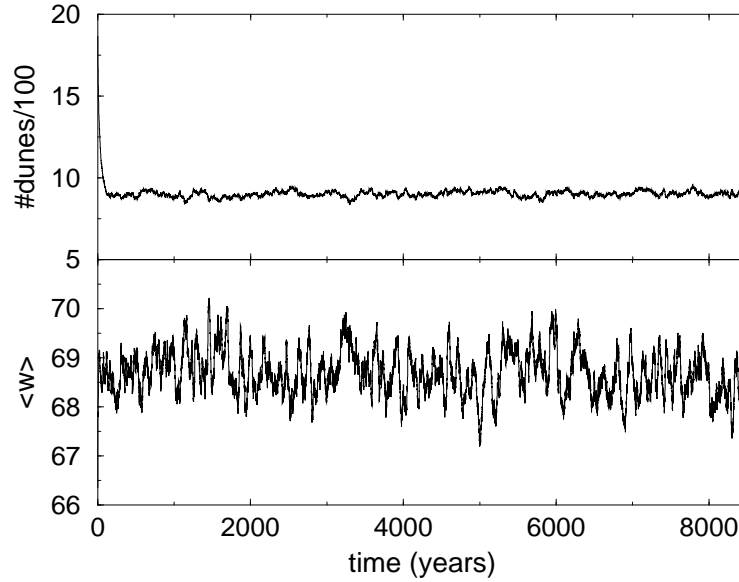


Fig. 6. Number and average size of dunes in the field

### 6.1 The confinement of the field

It is not clear up to now why real dune fields are typically confined on a stripe all the time. In our simple model, despite the fact that the diffusion of the sand tends to spread the sand to the borders, this behavior appears by itself. As seen in fig. 7, the sand flux decreases outside the central region of the field. Hence, dunes at the borders of that region receive less sand. The ones close to the center of the field receive more sand. This flux gradient acts like a “force” which pulls the dunes into the region where there is more flux, i.e. the central region where the other dunes are.

A way to see this effect is the distribution of dunes and their mean size at the end of the field. This is shown in figure (8). In the inset we plotted the number of dunes that leave the field at the right boundary. Near to the center of the field the dunes have approximately the same size, however the ones near to the borders are smaller, since they receive less sand. Since the dunes in the borders are smaller, they are faster and this explains why we have more dunes leaving the field close to the borders than in the center.

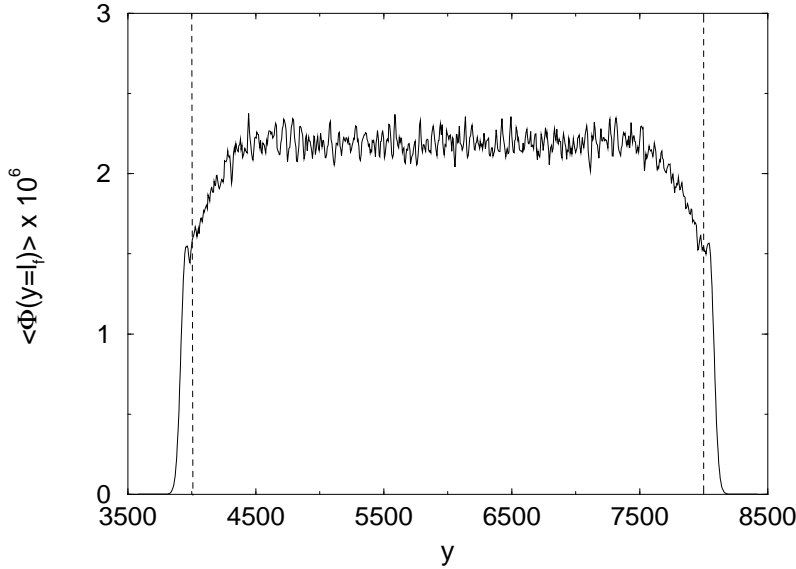


Fig. 7. Averaged flux at the end of the field.

### 6.2 Spatial correlations

Looking at fig. 1 we can observe that the dunes tend to form lines, the horn of one dune pointing to the center of the back of another one. These patterns are apparently due to the coupling through the inter-dune sand flux and we will show how they are reproduced by our model. In order to quantitatively

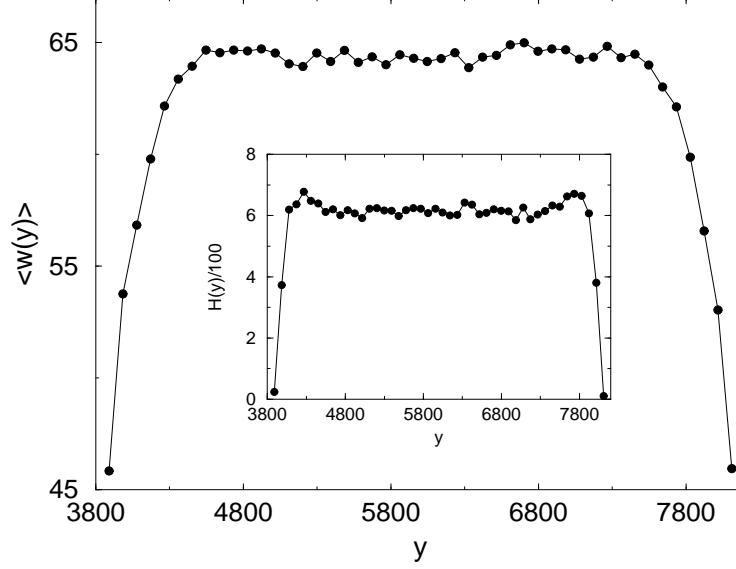


Fig. 8. Average size and number of dunes (inset) which leave a field of 50 km. We can see that the field stays confined and that the dunes outside of the central regions tend to shrink.

measure these structures, we will introduce two types of correlation functions which we will monitor as well in our model as also directly from a photograph of a real dune field in order to compare the patterns formed by our model to the observed ones.

Let us define the longitudinal correlation as

$$C_l(d) = \sum_i \sum_{j>i} \delta(d - |x_i - x_j|) \quad (18)$$

This function measures the correlation of dune positions in the wind direction.

In fig. 9 we present the results for our model. To get better statistics we take the average over several thousand time-steps. We observe very pronounced peaks at regular distances of about 50 m showing a characteristic distance between the dunes in wind direction.

It is also interesting to calculate the angular correlations in the positions of the dunes which can be quantified by the angular correlation function

$$C_p(\theta) = \sum_i \sum_{j>i} \delta \left( \theta - \arctan \left( \frac{y_i - y_j}{x_i - x_j} \right) \right) \quad (19)$$

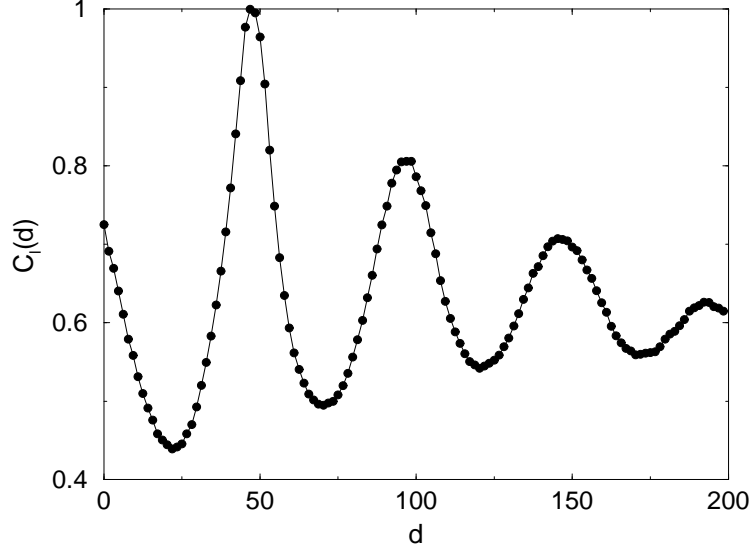


Fig. 9. Correlations in the wind direction obtained from our model after averaging over time.

where  $i$  and  $j$  are only chosen within the central part of the stripe (about one third of all dunes) in order to avoid boundary effects and for which the distance  $(x_i - x_j)^2 + (y_i - y_j)^2 < (5\text{km})^2$ . In fig. 10 we see our results for  $C_p(\theta)$  as obtained after averaging over all dunes in the central part of the field and several thousand time-steps.

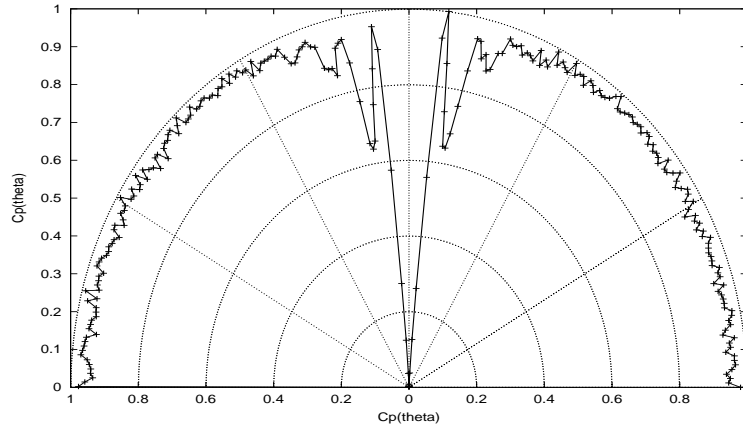


Fig. 10. Polar plot of the angular correlation  $C_p(\theta)$  between the dunes.

We see that while most directions have no particular structure in the forward direction there are two favorite directions symmetrical around the exact wind direction ( $x$ -axis) of high correlation. In the wind direction itself the correlation is particularly low. The selected direction corresponds to the arrangements where the dune in front is just shifted by half a dune width, so that the horns directly point to the center of the dune in front. Such configurations can be recognized with the naked eye on the photo of fig. 1.

## 7 Results from the experiments

We analysed aerial photos of the dune field of Laâyoune in Southern Morocco and obtained the position of 734 dunes as shown in fig. 11. In figs. 12 and 13 we show our results for both correlation functions corresponding to the correlation functions obtained for the model in figs. 9 and 10. Comparing figs. 9 and 12 one sees that the measured longitudinal correlation does not show much periodicity or characteristic distance. We believe that this lack of structure is rather due to insufficient statistics. After all the model gives the possibility to the average over time while the measurements are obtained from a single photo.

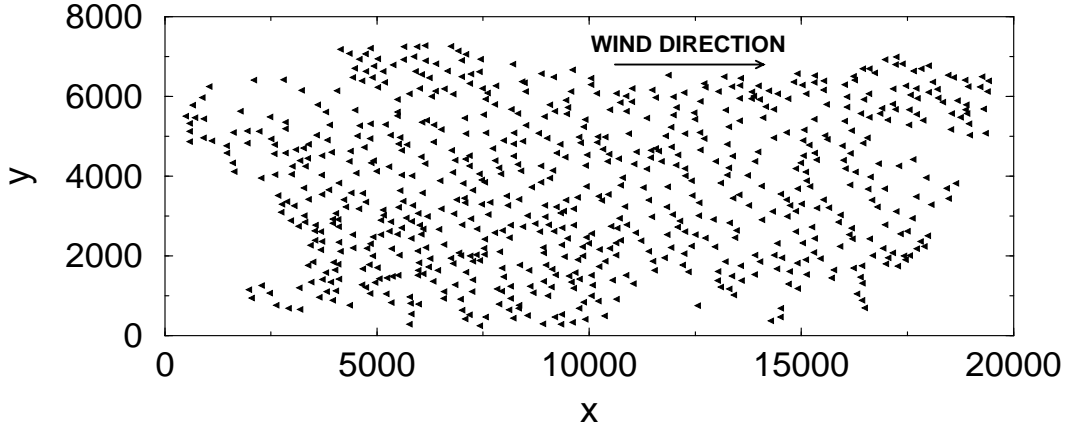


Fig. 11. Position of the dunes in the Barchan field of Laâyoune obtained from an aerial photo.

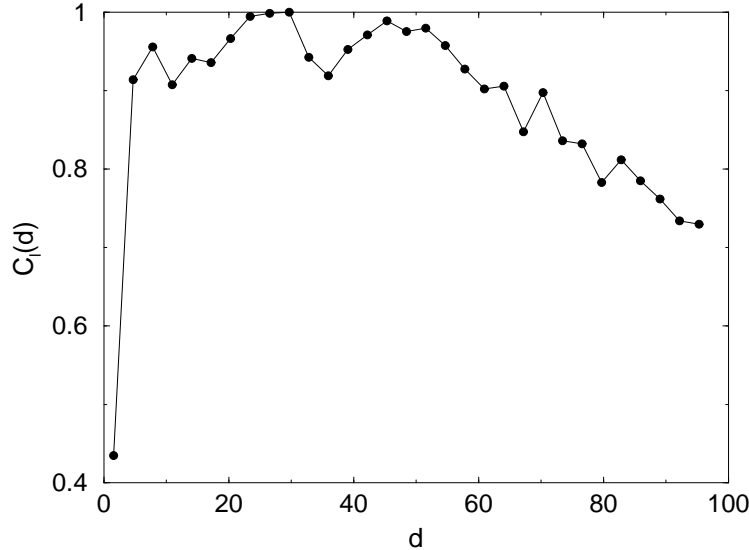


Fig. 12. Correlations in the wind direction obtained from the positions of the dunes in fig. 11.

Concerning the polar correlations, fig. 13 clearly shows the same two peaks

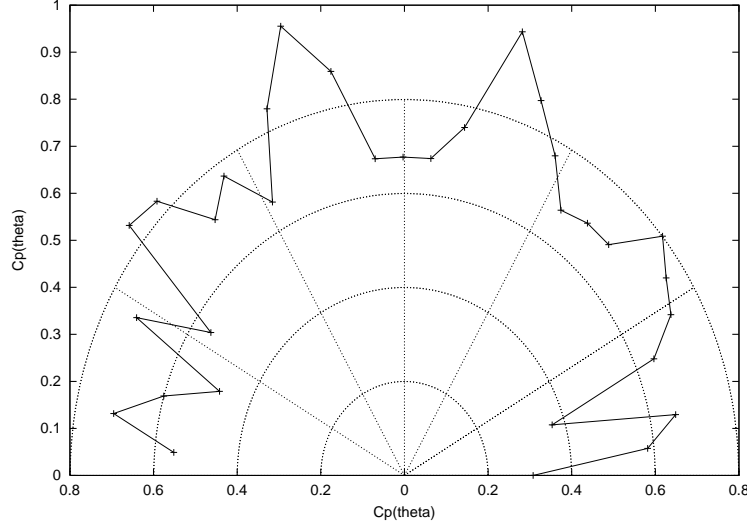


Fig. 13. Polar plot of the angular correlations  $C_p(\theta)$  of the dune field of Laâyoune.

pointing in both directions with an angle of  $\theta$  from the wind direction. But while in the model  $\theta$  was about  $8^\circ$ , it is about  $15^\circ$  for the real data.

## 8 Conclusions

In this paper we introduced a simple model for a field of Barchan dunes. The dunes are characterized by their width and position in the field. The model includes a diffusion of the sand. Assuming a simple law for the inter-dune sand flux we could show that the simulated field is stably confined and presents the same kind of spatial correlations as real fields.

An extension of this work could be to introduce variations in the wind direction. This could help to explain more complex patterns observed in deserts.

## 9 Acknowledgement

ARL acknowledges a fellowship from CNPq (Brazilian Agency) and Gerd Sauermann a fellowship from DAAD.

## References

- [1] S. Berne, J. F. Bourillet, J. Durand, and G. Lericolais. Les dunes subtidales géantes de Surtainville (manche ouest). *Bull. Centres Rech. Explor. Prod. Elf Aquitaine*, 13:395–415, 1989.
- [2] P. C. Thomas, M. C. Malin, M. H. Carr, G. E. Danielson, M. E. Davies, W. K. Hartmann, A. P. Ingersoll, P. B. James, A. S. Mcewen, L. A. Soderblom, and J. Veverka. Bright dunes on mars. *Nature*, 397:592–594, 1999.
- [3] H. J. Finkel. The barchans of southern Peru. *Journal of Geology*, 67:614–647, 1959.
- [4] S. Hastenrath. The barchans of the Arequipa region, southern Peru. *Zeitschrift für Geomorphologie*, 11:300–331, 1967.
- [5] S. Hastenrath. The barchan dunes of southern Peru revisited. *Zeitschrift für Geomorphologie*, 31-2:167–178, 1987.
- [6] K. Lettau and H. Lettau. Bulk transport of sand by the barchans of the Pampa de La Joya in southern Peru. *Zeitschrift für Geomorphologie N.F.*, 13-2:182–195, 1969.
- [7] K. Lettau and H. Lettau. Experimental and micrometeorological field studies of dune migration. In H. H. Lettau and K. Lettau, editors, *Exploring the world's driest climate*. Madison, Center for Climatic Research, Univ. Wisconsin, 1978.
- [8] G. Sauermann, P. Rognon, A. Poliakov, and H. J. Herrmann. The shape of the barchan dunes of southern Morocco. *Geomorphology*, 36:47–62, 2000.
- [9] K. Pye and H. Tsoar. *Aeolian sand and sand dunes*. Unwin Hyman, London, 1990.
- [10] R. A. Bagnold. *The physics of blown sand and desert dunes*. Methuen, London, 1941.
- [11] K. R. Rasmussen and H. E. Mikkelsen. Wind tunnel observations of aeolian transport rates. *Acta Mechanica*, Suppl 1:135–144, 1991.
- [12] G. Sauermann, K. Kroy, and H. J. Herrmann. A continuum saltation model for sand dunes. *Phys. Rev. E* 64, 31305 (2001).
- [13] P. S. Jackson and J. C. R. Hunt. Turbulent wind flow over a low hill. *Q. J. R. Meteorol. Soc.*, 101:929, 1975.
- [14] J. C. R. Hunt, S. Leibovich, and K. J. Richards. Turbulent wind flow over smooth hills. *Q. J. R. Meteorol. Soc.*, 114:1435–1470, 1988.
- [15] K. Kroy, G. Sauermann, and H. J. Herrmann. A minimal model for sand dunes. cond-mat/0101380, 2001.
- [16] G. Sauermann. *Modeling of Wind Blown Sand and Desert Dunes*. PhD thesis, University of Stuttgart, 2001.